

Measurement of CP Violation Parameters with a Dalitz Plot Analysis of $B^{\pm} \rightarrow D_{\pi^+ \pi^- \pi^0} K^{\pm}$

B. Aubert,¹ M. Bona,¹ D. Boutigny,¹ Y. Karyotakis,¹ J. P. Lees,¹ V. Poireau,¹ X. Prudent,¹ V. Tisserand,¹ A. Zghiche,¹ E. Grauges,² L. Lopez,³ A. Palano,³ J. C. Chen,⁴ N. D. Qi,⁴ G. Rong,⁴ P. Wang,⁴ Y. S. Zhu,⁴ G. Eigen,⁵ I. Ofte,⁵ B. Stugu,⁵ G. S. Abrams,⁶ M. Battaglia,⁶ D. N. Brown,⁶ J. Button-Shafer,⁶ R. N. Cahn,⁶ Y. Groysman,⁶ R. G. Jacobsen,⁶ J. A. Kadyk,⁶ L. T. Kerth,⁶ Yu. G. Kolomensky,⁶ G. Kukartsev,⁶ D. Lopes Pegna,⁶ G. Lynch,⁶ L. M. Mir,⁶ T. J. Orimoto,⁶ M. Pripstein,⁶ N. A. Roe,⁶ M. T. Ronan,^{6,*} K. Tackmann,⁶ W. A. Wenzel,⁶ P. del Amo Sanchez,⁷ M. Barrett,⁷ T. J. Harrison,⁷ A. J. Hart,⁷ C. M. Hawkes,⁷ A. T. Watson,⁷ T. Held,⁸ H. Koch,⁸ B. Lewandowski,⁸ M. Pelizaeus,⁸ T. Schroeder,⁸ M. Steinke,⁸ J. T. Boyd,⁹ J. P. Burke,⁹ W. N. Cottingham,⁹ D. Walker,⁹ D. J. Asgeirsson,¹⁰ T. Cuhadar-Donszelmann,¹⁰ B. G. Fulsom,¹⁰ C. Hearty,¹⁰ N. S. Knecht,¹⁰ T. S. Mattison,¹⁰ J. A. McKenna,¹⁰ A. Khan,¹¹ P. Kyberd,¹¹ M. Saleem,¹¹ D. J. Sherwood,¹¹ L. Teodorescu,¹¹ V. E. Blinov,¹² A. D. Bukin,¹² V. P. Druzhinin,¹² V. B. Golubev,¹² A. P. Onuchin,¹² S. I. Serednyakov,¹² Yu. I. Skovpen,¹² E. P. Solodov,¹² K. Yu Todyshev,¹² M. Bondioli,¹³ M. Bruinsma,¹³ M. Chao,¹³ S. Curry,¹³ I. Eschrich,¹³ D. Kirkby,¹³ A. J. Lankford,¹³ P. Lund,¹³ M. Mandelkern,¹³ E. C. Martin,¹³ D. P. Stoker,¹³ S. Abachi,¹⁴ C. Buchanan,¹⁴ S. D. Foulkes,¹⁵ J. W. Gary,¹⁵ F. Liu,¹⁵ O. Long,¹⁵ B. C. Shen,¹⁵ L. Zhang,¹⁵ E. J. Hill,¹⁶ H. P. Paar,¹⁶ S. Rahatlou,¹⁶ V. Sharma,¹⁶ J. W. Berryhill,¹⁷ C. Campagnari,¹⁷ A. Cunha,¹⁷ B. Dahmes,¹⁷ T. M. Hong,¹⁷ D. Kovalskyi,¹⁷ J. D. Richman,¹⁷ T. W. Beck,¹⁸ A. M. Eisner,¹⁸ C. J. Flacco,¹⁸ C. A. Heusch,¹⁸ J. Kroseberg,¹⁸ W. S. Lockman,¹⁸ T. Schalk,¹⁸ B. A. Schumm,¹⁸ A. Seiden,¹⁸ D. C. Williams,¹⁸ M. G. Wilson,¹⁸ L. O. Winstrom,¹⁸ E. Chen,¹⁹ C. H. Cheng,¹⁹ A. Dvoretzkii,¹⁹ F. Fang,¹⁹ D. G. Hitlin,¹⁹ I. Narsky,¹⁹ T. Piatenko,¹⁹ F. C. Porter,¹⁹ G. Mancinelli,²⁰ B. T. Meadows,²⁰ K. Mishra,²⁰ M. D. Sokoloff,²⁰ F. Blanc,²¹ P. C. Bloom,²¹ S. Chen,²¹ W. T. Ford,²¹ J. F. Hirschauer,²¹ A. Kreisel,²¹ M. Nagel,²¹ U. Nauenberg,²¹ A. Olivas,²¹ J. G. Smith,²¹ K. A. Ulmer,²¹ S. R. Wagner,²¹ J. Zhang,²¹ A. Chen,²² E. A. Eckhart,²² A. Soffer,^{22,†} W. H. Toki,²² R. J. Wilson,²² F. Winklmeier,²² Q. Zeng,²² D. D. Altenburg,²³ E. Feltresi,²³ A. Hauke,²³ H. Jasper,²³ J. Merkel,²³ A. Petzold,²³ B. Spaan,²³ K. Wacker,²³ T. Brandt,²⁴ V. Klose,²⁴ H. M. Lacker,²⁴ W. F. Mader,²⁴ R. Nogowski,²⁴ J. Schubert,²⁴ K. R. Schubert,²⁴ R. Schwierz,²⁴ J. E. Sundermann,²⁴ A. Volk,²⁴ D. Bernard,²⁵ G. R. Bonneaud,²⁵ E. Latour,²⁵ Ch. Thiebaux,²⁵ M. Verderi,²⁵ P. J. Clark,²⁶ W. Gradl,²⁶ F. Muheim,²⁶ S. Playfer,²⁶ A. I. Robertson,²⁶ Y. Xie,²⁶ M. Andreotti,²⁷ D. Bettoni,²⁷ C. Bozzi,²⁷ R. Calabrese,²⁷ G. Cibinetto,²⁷ E. Luppi,²⁷ M. Negrini,²⁷ A. Petrella,²⁷ L. Piemontese,²⁷ E. Prencipe,²⁷ F. Anulli,²⁸ R. Baldini-Ferroli,²⁸ A. Calcaterra,²⁸ R. de Sangro,²⁸ G. Finocchiaro,²⁸ S. Pacetti,²⁸ P. Patteri,²⁸ I. M. Peruzzi,^{28,‡} M. Piccolo,²⁸ M. Rama,²⁸ A. Zallo,²⁸ A. Buzzo,²⁹ R. Contri,²⁹ M. Lo Vetere,²⁹ M. M. Macri,²⁹ M. R. Monge,²⁹ S. Passaggio,²⁹ C. Patrignani,²⁹ E. Robutti,²⁹ A. Santroni,²⁹ S. Tosi,²⁹ K. S. Chaisanguanthum,³⁰ M. Morii,³⁰ J. Wu,³⁰ R. S. Dubitzky,³¹ J. Marks,³¹ S. Schenk,³¹ U. Uwer,³¹ D. J. Bard,³² P. D. Dauncey,³² R. L. Flack,³² J. A. Nash,³² M. B. Nikolich,³² W. Panduro Vazquez,³² P. K. Behera,³³ X. Chai,³³ M. J. Charles,³³ U. Mallik,³³ N. T. Meyer,³³ V. Ziegler,³³ J. Cochran,³⁴ H. B. Crawley,³⁴ L. Dong,³⁴ V. Eyges,³⁴ W. T. Meyer,³⁴ S. Prell,³⁴ E. I. Rosenberg,³⁴ A. E. Rubin,³⁴ A. V. Gritsan,³⁵ C. K. Lae,³⁵ A. G. Denig,³⁶ M. Fritsch,³⁶ G. Schott,³⁶ N. Arnaud,³⁷ J. Béquilleux,³⁷ M. Davier,³⁷ G. Grosdidier,³⁷ A. Höcker,³⁷ V. Lepeltier,³⁷ F. Le Diberder,³⁷ A. M. Lutz,³⁷ S. Pruvot,³⁷ S. Rodier,³⁷ P. Roudeau,³⁷ M. H. Schune,³⁷ J. Serrano,³⁷ V. Sordini,³⁷ A. Stocchi,³⁷ W. F. Wang,³⁷ G. Wormser,³⁷ D. J. Lange,³⁸ D. M. Wright,³⁸ C. A. Chavez,³⁹ I. J. Forster,³⁹ J. R. Fry,³⁹ E. Gabathuler,³⁹ R. Gamet,³⁹ D. E. Hutchcroft,³⁹ D. J. Payne,³⁹ K. C. Schofield,³⁹ C. Touramanis,³⁹ A. J. Bevan,⁴⁰ K. A. George,⁴⁰ F. Di Lodovico,⁴⁰ W. Menges,⁴⁰ R. Sacco,⁴⁰ G. Cowan,⁴¹ H. U. Flaecher,⁴¹ D. A. Hopkins,⁴¹ P. S. Jackson,⁴¹ T. R. McMahon,⁴¹ F. Salvatore,⁴¹ A. C. Wren,⁴¹ D. N. Brown,⁴² C. L. Davis,⁴² J. Allison,⁴³ N. R. Barlow,⁴³ R. J. Barlow,⁴³ Y. M. Chia,⁴³ C. L. Edgar,⁴³ G. D. Lafferty,⁴³ T. J. West,⁴³ J. I. Yi,⁴³ C. Chen,⁴⁴ W. D. Hulsbergen,⁴⁴ A. Jawahery,⁴⁴ D. A. Roberts,⁴⁴ G. Simi,⁴⁴ G. Blaylock,⁴⁵ C. Dallapiccola,⁴⁵ S. S. Hertzbach,⁴⁵ X. Li,⁴⁵ T. B. Moore,⁴⁵ E. Salvati,⁴⁵ S. Saremi,⁴⁵ R. Cowan,⁴⁶ G. Sciolla,⁴⁶ S. J. Sekula,⁴⁶ M. Spitznagel,⁴⁶ F. Taylor,⁴⁶ R. K. Yamamoto,⁴⁶ H. Kim,⁴⁷ S. E. Mclachlin,⁴⁷ P. M. Patel,⁴⁷ S. H. Robertson,⁴⁷ A. Lazzaro,⁴⁸ V. Lombardo,⁴⁸ F. Palombo,⁴⁸ J. M. Bauer,⁴⁹ L. Cremaldi,⁴⁹ V. Eschenburg,⁴⁹ R. Godang,⁴⁹ R. Kroeger,⁴⁹ D. A. Sanders,⁴⁹ D. J. Summers,⁴⁹ H. W. Zhao,⁴⁹ S. Brunet,⁵⁰ D. Côté,⁵⁰ M. Simard,⁵⁰ P. Taras,⁵⁰ F. B. Viaud,⁵⁰ H. Nicholson,⁵¹ N. Cavallo,^{52,§} G. De Nardo,⁵² F. Fabozzi,^{52,§} C. Gatto,⁵² L. Lista,⁵² D. Monorchio,⁵² P. Paolucci,⁵² D. Piccolo,⁵² C. Sciacca,⁵² M. A. Baak,⁵³ G. Raven,⁵³ H. L. Snoek,⁵³ C. P. Jessop,⁵⁴ J. M. LoSecco,⁵⁴ G. Benelli,⁵⁵ L. A. Corwin,⁵⁵ K. K. Gan,⁵⁵ K. Honscheid,⁵⁵ D. Hufnagel,⁵⁵ H. Kagan,⁵⁵ R. Kass,⁵⁵ J. P. Morris,⁵⁵ A. M. Rahimi,⁵⁵ J. J. Regensburger,⁵⁵ R. Ter-Antonyan,⁵⁵ Q. K. Wong,⁵⁵ N. L. Blount,⁵⁶ J. Brau,⁵⁶ R. Frey,⁵⁶ O. Igonkina,⁵⁶ J. A. Kolb,⁵⁶ M. Lu,⁵⁶ R. Rahmat,⁵⁶ N. B. Sinev,⁵⁶ D. Strom,⁵⁶ J. Strube,⁵⁶ E. Torrence,⁵⁶ A. Gaz,⁵⁷ M. Margoni,⁵⁷ M. Morandin,⁵⁷ A. Pompili,⁵⁷ M. Posocco,⁵⁷ M. Rotondo,⁵⁷ F. Simonetto,⁵⁷ R. Stroili,⁵⁷ C. Voci,⁵⁷ E. Ben-Haim,⁵⁸ H. Briand,⁵⁸ J. Chauveau,⁵⁸ P. David,⁵⁸ L. Del Buono,⁵⁸ Ch. de la Vaissière,⁵⁸ O. Hamon,⁵⁸

B. L. Hartfiel,⁵⁸ Ph. Leruste,⁵⁸ J. Malclès,⁵⁸ J. Ocariz,⁵⁸ A. Perez,⁵⁸ J. Prendki,⁵⁸ L. Gladney,⁵⁹ M. Biasini,⁶⁰ R. Covarelli,⁶⁰ E. Manoni,⁶⁰ C. Angelini,⁶¹ G. Batignani,⁶¹ S. Bettarini,⁶¹ G. Calderini,⁶¹ M. Carpinelli,⁶¹ R. Cenci,⁶¹ F. Forti,⁶¹ M. A. Giorgi,⁶¹ A. Lusiani,⁶¹ G. Marchiori,⁶¹ M. A. Mazur,⁶¹ M. Morganti,⁶¹ N. Neri,⁶¹ E. Paoloni,⁶¹ G. Rizzo,⁶¹ J. J. Walsh,⁶¹ M. Haire,⁶² J. Biesiada,⁶³ P. Elmer,⁶³ Y. P. Lau,⁶³ C. Lu,⁶³ J. Olsen,⁶³ A. J. S. Smith,⁶³ A. V. Telnov,⁶³ E. Baracchini,⁶⁴ F. Bellini,⁶⁴ G. Cavoto,⁶⁴ A. D'Orazio,⁶⁴ D. del Re,⁶⁴ E. Di Marco,⁶⁴ R. Faccini,⁶⁴ F. Ferrarotto,⁶⁴ F. Ferroni,⁶⁴ M. Gaspero,⁶⁴ P. D. Jackson,⁶⁴ L. Li Gioi,⁶⁴ M. A. Mazzoni,⁶⁴ S. Morganti,⁶⁴ G. Piredda,⁶⁴ F. Polci,⁶⁴ F. Renga,⁶⁴ C. Voena,⁶⁴ M. Ebert,⁶⁵ H. Schröder,⁶⁵ R. Waldi,⁶⁵ T. Adye,⁶⁶ G. Castelli,⁶⁶ B. Franek,⁶⁶ E. O. Olaiya,⁶⁶ S. Ricciardi,⁶⁶ W. Roethel,⁶⁶ F. F. Wilson,⁶⁶ R. Aleksan,⁶⁷ S. Emery,⁶⁷ M. Escalier,⁶⁷ A. Gaidot,⁶⁷ S. F. Ganzhur,⁶⁷ G. Hamel de Monchenault,⁶⁷ W. Kozanecki,⁶⁷ M. Legendre,⁶⁷ G. Vasseur,⁶⁷ Ch. Yèche,⁶⁷ M. Zito,⁶⁷ X. R. Chen,⁶⁸ H. Liu,⁶⁸ W. Park,⁶⁸ M. V. Purohit,⁶⁸ J. R. Wilson,⁶⁸ M. T. Allen,⁶⁹ D. Aston,⁶⁹ R. Bartoldus,⁶⁹ P. Bechtle,⁶⁹ N. Berger,⁶⁹ R. Claus,⁶⁹ J. P. Coleman,⁶⁹ M. R. Convery,⁶⁹ J. C. Dingfelder,⁶⁹ J. Dorfan,⁶⁹ G. P. Dubois-Felsmann,⁶⁹ D. Dujmic,⁶⁹ W. Dunwoodie,⁶⁹ R. C. Field,⁶⁹ T. Glanzman,⁶⁹ S. J. Gowdy,⁶⁹ M. T. Graham,⁶⁹ P. Grenier,⁶⁹ V. Halyo,⁶⁹ C. Hast,⁶⁹ T. Hryn'ova,⁶⁹ W. R. Innes,⁶⁹ M. H. Kelsey,⁶⁹ P. Kim,⁶⁹ D. W. G. S. Leith,⁶⁹ S. Li,⁶⁹ S. Luitz,⁶⁹ V. Luth,⁶⁹ H. L. Lynch,⁶⁹ D. B. MacFarlane,⁶⁹ H. Marsiske,⁶⁹ R. Messner,⁶⁹ D. R. Muller,⁶⁹ C. P. O'Grady,⁶⁹ V. E. Ozcan,⁶⁹ A. Perazzo,⁶⁹ M. Perl,⁶⁹ T. Pulliam,⁶⁹ B. N. Ratcliff,⁶⁹ A. Roodman,⁶⁹ A. A. Salnikov,⁶⁹ R. H. Schindler,⁶⁹ J. Schwiening,⁶⁹ A. Snyder,⁶⁹ J. Stelzer,⁶⁹ D. Su,⁶⁹ M. K. Sullivan,⁶⁹ K. Suzuki,⁶⁹ S. K. Swain,⁶⁹ J. M. Thompson,⁶⁹ J. Va'vra,⁶⁹ N. van Bakel,⁶⁹ A. P. Wagner,⁶⁹ M. Weaver,⁶⁹ W. J. Wisniewski,⁶⁹ M. Wittgen,⁶⁹ D. H. Wright,⁶⁹ H. W. Wulsin,⁶⁹ A. K. Yarritu,⁶⁹ K. Yi,⁶⁹ C. C. Young,⁶⁹ P. R. Burchat,⁷⁰ A. J. Edwards,⁷⁰ S. A. Majewski,⁷⁰ B. A. Petersen,⁷⁰ L. Wilden,⁷⁰ S. Ahmed,⁷¹ M. S. Alam,⁷¹ R. Bula,⁷¹ J. A. Ernst,⁷¹ V. Jain,⁷¹ B. Pan,⁷¹ M. A. Saeed,⁷¹ F. R. Wappler,⁷¹ S. B. Zain,⁷¹ W. Bugg,⁷² M. Krishnamurthy,⁷² S. M. Spanier,⁷² R. Eckmann,⁷³ J. L. Ritchie,⁷³ C. J. Schilling,⁷³ R. F. Schwitters,⁷³ J. M. Izen,⁷⁴ X. C. Lou,⁷⁴ S. Ye,⁷⁴ F. Bianchi,⁷⁵ F. Gallo,⁷⁵ D. Gamba,⁷⁵ M. Pelliccioni,⁷⁵ M. Bomben,⁷⁶ L. Bosisio,⁷⁶ C. Cartaro,⁷⁶ F. Cossutti,⁷⁶ G. Della Ricca,⁷⁶ L. Lanceri,⁷⁶ L. Vitale,⁷⁶ V. Azzolini,⁷⁷ N. Lopez-March,⁷⁷ F. Martinez-Vidal,⁷⁷ A. Oyanguren,⁷⁷ J. Albert,⁷⁸ Sw. Banerjee,⁷⁸ B. Bhuyan,⁷⁸ K. Hamano,⁷⁸ R. Kowalewski,⁷⁸ I. M. Nugent,⁷⁸ J. M. Roney,⁷⁸ R. J. Sobie,⁷⁸ J. J. Back,⁷⁹ P. F. Harrison,⁷⁹ T. E. Latham,⁷⁹ G. B. Mohanty,⁷⁹ M. Pappagallo,⁷⁹ H. R. Band,⁸⁰ X. Chen,⁸⁰ S. Dasu,⁸⁰ K. T. Flood,⁸⁰ J. J. Hollar,⁸⁰ P. E. Kutter,⁸⁰ B. Mellado,⁸⁰ Y. Pan,⁸⁰ M. Pierini,⁸⁰ R. Prepost,⁸⁰ S. L. Wu,⁸⁰ Z. Yu,⁸⁰ and H. Neal⁸¹

(BABAR Collaboration)

¹Laboratoire de Physique des Particules, IN2P3/CNRS et Université de Savoie, F-74941 Annecy-Le-Vieux, France

²Facultat de Física, Departament ECM, Universitat de Barcelona, E-08028 Barcelona, Spain

³Dipartimento di Fisica and INFN, Università di Bari, I-70126 Bari, Italy

⁴Institute of High Energy Physics, Beijing 100039, China

⁵Institute of Physics, University of Bergen, N-5007 Bergen, Norway

⁶Lawrence Berkeley National Laboratory and University of California, Berkeley, California 94720, USA

⁷University of Birmingham, Birmingham, B15 2TT, United Kingdom

⁸Institut für Experimentalphysik I, Ruhr Universität Bochum, D-44780 Bochum, Germany

⁹University of Bristol, Bristol BS8 1TL, United Kingdom

¹⁰University of British Columbia, Vancouver, British Columbia, Canada V6T 1Z1

¹¹Brunel University, Uxbridge, Middlesex UB8 3PH, United Kingdom

¹²Budker Institute of Nuclear Physics, Novosibirsk 630090, Russia

¹³University of California at Irvine, Irvine, California 92697, USA

¹⁴University of California at Los Angeles, Los Angeles, California 90024, USA

¹⁵University of California at Riverside, Riverside, California 92521, USA

¹⁶University of California at San Diego, La Jolla, California 92093, USA

¹⁷University of California at Santa Barbara, Santa Barbara, California 93106, USA

¹⁸Institute for Particle Physics, University of California at Santa Cruz, Santa Cruz, California 95064, USA

¹⁹California Institute of Technology, Pasadena, California 91125, USA

²⁰University of Cincinnati, Cincinnati, Ohio 45221, USA

²¹University of Colorado, Boulder, Colorado 80309, USA

²²Colorado State University, Fort Collins, Colorado 80523, USA

²³Institut für Physik, Universität Dortmund, D-44221 Dortmund, Germany

²⁴Institut für Kern- und Teilchenphysik, Technische Universität Dresden, D-01062 Dresden, Germany

²⁵Laboratoire Leprince-Ringuet, CNRS/IN2P3, Ecole Polytechnique, F-91128 Palaiseau, France

²⁶University of Edinburgh, Edinburgh EH9 3JZ, United Kingdom

- ²⁷*Dipartimento di Fisica and INFN, Università di Ferrara, I-44100 Ferrara, Italy*
- ²⁸*Laboratori Nazionali di Frascati dell'INFN, I-00044 Frascati, Italy*
- ²⁹*Dipartimento di Fisica and INFN, Università di Genova, I-16146 Genova, Italy*
- ³⁰*Harvard University, Cambridge, Massachusetts 02138, USA*
- ³¹*Physikalisches Institut, Universität Heidelberg, Philosophenweg 12, D-69120 Heidelberg, Germany*
- ³²*Imperial College London, London, SW7 2AZ, United Kingdom*
- ³³*University of Iowa, Iowa City, Iowa 52242, USA*
- ³⁴*Iowa State University, Ames, Iowa 50011-3160, USA*
- ³⁵*Johns Hopkins University, Baltimore, Maryland 21218, USA*
- ³⁶*Institut für Experimentelle Kernphysik, Universität Karlsruhe, D-76021 Karlsruhe, Germany*
- ³⁷*Laboratoire de l'Accélérateur Linéaire, IN2P3/CNRS et Université Paris-Sud 11, Centre Scientifique d'Orsay, B. P. 34, F-91898 ORSAY Cedex, France*
- ³⁸*Lawrence Livermore National Laboratory, Livermore, California 94550, USA*
- ³⁹*University of Liverpool, Liverpool L69 7ZE, United Kingdom*
- ⁴⁰*Queen Mary, University of London, E1 4NS, United Kingdom*
- ⁴¹*University of London, Royal Holloway and Bedford New College, Egham, Surrey TW20 0EX, United Kingdom*
- ⁴²*University of Louisville, Louisville, Kentucky 40292, USA*
- ⁴³*University of Manchester, Manchester M13 9PL, United Kingdom*
- ⁴⁴*University of Maryland, College Park, Maryland 20742, USA*
- ⁴⁵*University of Massachusetts, Amherst, Massachusetts 01003, USA*
- ⁴⁶*Laboratory for Nuclear Science, Massachusetts Institute of Technology, Cambridge, Massachusetts 02139, USA*
- ⁴⁷*McGill University, Montréal, Québec, Canada H3A 2T8*
- ⁴⁸*Dipartimento di Fisica and INFN, Università di Milano, I-20133 Milano, Italy*
- ⁴⁹*University of Mississippi, University, Mississippi 38677, USA*
- ⁵⁰*Physique des Particules, Université de Montréal, Montréal, Québec, Canada H3C 3J7*
- ⁵¹*Mount Holyoke College, South Hadley, Massachusetts 01075, USA*
- ⁵²*Dipartimento di Scienze Fisiche and INFN, Università di Napoli Federico II, I-80126, Napoli, Italy*
- ⁵³*NIKHEF, National Institute for Nuclear Physics and High Energy Physics, NL-1009 DB Amsterdam, The Netherlands*
- ⁵⁴*University of Notre Dame, Notre Dame, Indiana 46556, USA*
- ⁵⁵*Ohio State University, Columbus, Ohio 43210, USA*
- ⁵⁶*University of Oregon, Eugene, Oregon 97403, USA*
- ⁵⁷*Dipartimento di Fisica and INFN, Università di Padova, I-35131 Padova, Italy*
- ⁵⁸*Laboratoire de Physique Nucléaire et de Hautes Energies, IN2P3/CNRS, Université Pierre et Marie Curie-Paris6, Université Denis Diderot-Paris7, F-75252 Paris, France*
- ⁵⁹*University of Pennsylvania, Philadelphia, Pennsylvania 19104, USA*
- ⁶⁰*Dipartimento di Fisica and INFN, Università di Perugia, I-06100 Perugia, Italy*
- ⁶¹*Dipartimento di Fisica, Scuola Normale Superiore, and INFN, Università di Pisa, I-56127 Pisa, Italy*
- ⁶²*Prairie View A&M University, Prairie View, Texas 77446, USA*
- ⁶³*Princeton University, Princeton, New Jersey 08544, USA*
- ⁶⁴*Dipartimento di Fisica and INFN, Università di Roma La Sapienza, I-00185 Roma, Italy*
- ⁶⁵*Universität Rostock, D-18051 Rostock, Germany*
- ⁶⁶*Rutherford Appleton Laboratory, Chilton, Didcot, Oxon, OX11 0QX, United Kingdom*
- ⁶⁷*DSM/Dapnia, CEA/Saclay, F-91191 Gif-sur-Yvette, France*
- ⁶⁸*University of South Carolina, Columbia, South Carolina 29208, USA*
- ⁶⁹*Stanford Linear Accelerator Center, Stanford, California 94309, USA*
- ⁷⁰*Stanford University, Stanford, California 94305-4060, USA*
- ⁷¹*State University of New York, Albany, New York 12222, USA*
- ⁷²*University of Tennessee, Knoxville, Tennessee 37996, USA*
- ⁷³*University of Texas at Austin, Austin, Texas 78712, USA*
- ⁷⁴*University of Texas at Dallas, Richardson, Texas 75083, USA*
- ⁷⁵*Dipartimento di Fisica Sperimentale and INFN, Università di Torino, I-10125 Torino, Italy*
- ⁷⁶*Dipartimento di Fisica and INFN, Università di Trieste, I-34127 Trieste, Italy*
- ⁷⁷*IFIC, Universitat de Valencia-CSIC, E-46071 Valencia, Spain*
- ⁷⁸*University of Victoria, Victoria, British Columbia, Canada V8W 3P6*
- ⁷⁹*Department of Physics, University of Warwick, Coventry CV4 7AL, United Kingdom*
- ⁸⁰*University of Wisconsin, Madison, Wisconsin 53706, USA*
- ⁸¹*Yale University, New Haven, Connecticut 06511, USA*

(Received 23 March 2007; published 17 December 2007)

We report the results of a CP violation analysis of the decay $B^\pm \rightarrow D_{\pi^+\pi^-\pi^0} K^\pm$, where $D_{\pi^+\pi^-\pi^0}$ indicates a neutral D meson detected in the final state $\pi^+\pi^-\pi^0$, excluding $K_S^0\pi^0$. The analysis makes use

of $324 \times 10^6 e^+e^- \rightarrow B\bar{B}$ events recorded by the *BABAR* experiment at the PEP-II e^+e^- storage ring. Analyzing the $\pi^+\pi^-\pi^0$ Dalitz plot distribution and the $B^\pm \rightarrow D_{\pi^+\pi^-\pi^0}K^\pm$ branching fraction and decay rate asymmetry, we find the following one-standard-deviation constraints on the amplitude ratio and on the weak and strong phases: $0.06 < r_B < 0.78$, $-30^\circ < \gamma < 76^\circ$, $-27^\circ < \delta < 78^\circ$. We also measure the magnitudes and phases of the components of the $D^0 \rightarrow \pi^+\pi^-\pi^0$ decay amplitude.

DOI: 10.1103/PhysRevLett.99.251801

PACS numbers: 13.25.Hw, 12.15.Hh, 11.30.Er

An important component of the program to study *CP* violation is the measurement of the angle $\gamma = \arg(-V_{ud}V_{ub}^*/V_{cd}V_{cb}^*)$ of the unitarity triangle related to the Cabibbo-Kobayashi-Maskawa quark mixing matrix [1]. The decays $B \rightarrow D^{(*)0}K^{(*)}$ can be used to measure γ with essentially no hadronic uncertainties, exploiting interference between $b \rightarrow u\bar{c}s$ and $b \rightarrow c\bar{u}s$ decay amplitudes [2]. In one of the measurement methods [3], γ is extracted by analyzing the *D*-decay Dalitz plot distribution in $B^\pm \rightarrow DK^\pm$ with multibody *D* decays [4]. This method has only been used with the Cabibbo-favored decay $D \rightarrow K_S^0\pi^+\pi^-$ [5,6], and Cabibbo-suppressed decays are expected to be similarly sensitive to γ [7]. We present here the first *CP*-violation study of $B^\pm \rightarrow DK^\pm$ with a multibody, Cabibbo-suppressed *D* decay, $D \rightarrow \pi^+\pi^-\pi^0$.

The data used in this analysis were collected with the *BABAR* detector at the PEP-II e^+e^- storage ring, and they include 288 fb^{-1} taken on the $\Upsilon(4S)$ resonance and 27 fb^{-1} collected 40 MeV below the resonance. Samples of simulated Monte Carlo (MC) events were analyzed with the same reconstruction and analysis procedures. These samples include an $e^+e^- \rightarrow B\bar{B}$ sample 5 times larger than the data, a continuum $e^+e^- \rightarrow q\bar{q}$ sample, where *q* is a *u*, *d*, *s*, or *c* quark, with luminosity equivalent to the data, and a signal sample 300 times larger than the data, with both phase space *D* decays and decays generated according to the amplitudes measured by CLEO [8]. The *BABAR* detector and the methods used for particle reconstruction and identification are described in Ref. [9].

We use event-shape variables [10] to suppress the continuum background, and we identify kaon and pion candidates using specific ionization and Cherenkov radiation. The invariant mass of *D* candidates must satisfy $1830 < M_D < 1895 \text{ MeV}/c^2$. We require $5272 < m_{\text{ES}} < 5300 \text{ MeV}/c^2$, where $m_{\text{ES}} \equiv \sqrt{E_{\text{c.m.}}^2/4 - |\mathbf{p}_B|^2}$, $E_{\text{c.m.}}$ is the total e^+e^- center of mass (c.m.) energy, and \mathbf{p}_B is the *B* candidate c.m. momentum. Events must satisfy $-70 < \Delta E < 60 \text{ MeV}$, where $\Delta E = E_B - E_{\text{c.m.}}/2$ and E_B is the *B* candidate c.m. energy. We exclude the decay mode $D \rightarrow K_S^0\pi^0$, which is a previously studied *CP* eigenstate not related to the method of Ref. [3], by rejecting candidates with $489 < M(\pi^+\pi^-) < 508 \text{ MeV}/c^2$ or for which the distance between the $\pi^+\pi^-$ vertex and the *B* candidate decay vertex is more than 1.5 cm. We reject $B^\pm \rightarrow D_{\pi^+\pi^-\pi^0}K^\pm$ candidates in which the $K^\pm\pi^\mp$ invariant mass satisfies $1840 < M(K^\pm\pi^\mp) < 1890 \text{ MeV}/c^2$, to suppress $B^- \rightarrow D_{K^-\pi^+\rho^-}$ decays. We require $d > 0.25$,

where *d* [10] is a neural net variable that separates signal candidates (which peak toward $d = 1$) from those with a misreconstructed *D* (peaking toward $d = 0$). In events with multiple candidates (9% of the sample), we keep the candidate whose m_{ES} value is closest to the nominal B^\pm mass [11]. The final signal reconstruction efficiency is $\epsilon = 11.4\%$.

For each $B^\pm \rightarrow D_{\pi^+\pi^-\pi^0}K^\pm$ candidate, we compute the neural net variable *q* [10]. The *q* distribution of $B\bar{B}$ events peaks toward $q = 1$, while that of continuum peaks at $q = 0$. For $\nu \in \{q, d\}$, we define the variables $\nu' \equiv \tanh^{-1}[\nu - \frac{1}{2}(\nu_{\text{max}} + \nu_{\text{min}})] / \frac{1}{2}(\nu_{\text{max}} - \nu_{\text{min}})$, where $q_{\text{max}} = d_{\text{max}} = 1$, $q_{\text{min}} = 0.1$, and $d_{\text{min}} = 0.25$ are the allowed ranges for *q* and *d*. The ν' variables can be conveniently fit with Gaussians, as described later.

As in Ref. [10], we identify in the MC samples ten event types, one signal, and nine different backgrounds. We list them here with the labels used to refer to them throughout the Letter. **DK_{sig}**: $B^\pm \rightarrow D_{\pi^+\pi^-\pi^0}K^\pm$ events that are correctly reconstructed; these are the only events considered to be signal. **DK_{bgd}**: $B^\pm \rightarrow D_{\pi^+\pi^-\pi^0}K^\pm$ events that are misreconstructed; namely, some of the particles used to form the final state do not originate from the $B^\pm \rightarrow D_{\pi^+\pi^-\pi^0}K^\pm$ decay. **Dπ_D** (**Dπ_ϕ**): $B^- \rightarrow D^0\pi^-$, $D^0 \rightarrow \pi^+\pi^-\pi^0$ decays, where the decay $D^0 \rightarrow \pi^+\pi^-\pi^0$ is correctly reconstructed (misreconstructed). **DKX**: $B \rightarrow D^{(*)}K^{(*)-}$ events not containing the decay $D \rightarrow \pi^+\pi^-\pi^0$. **DπX**: $B \rightarrow D^{(*)}\pi^-$ and $B \rightarrow D^{(*)}\rho^-$ decays, excluding $D \rightarrow \pi^+\pi^-\pi^0$. **BBC_D** (**BBC_ϕ**): all other $B\bar{B}$ events with a correctly reconstructed (misreconstructed) *D* candidate. **qq_D** (**qq_ϕ**): continuum $e^+e^- \rightarrow q\bar{q}$ events with a correctly reconstructed (misreconstructed) *D* candidate.

The measurement of the *CP* parameters proceeds in three steps, each involving an unbinned maximum likelihood fit. In step 1, we measure the complex Dalitz plot amplitude $f(s_+, s_-)$ for the decay $D^0 \rightarrow \pi^+\pi^-\pi^0$, where $s_\pm = m^2(\pi^\pm\pi^0)$ are the squared invariant masses of the $\pi^\pm\pi^0$ pairs. In step 2, we extract the numbers of B^+ and B^- signal events and background yields. We obtain the *CP* parameters in step 3.

We parametrize $f(s_+, s_-)$ using the isobar model, $f(s_+, s_-) = [a_{\text{NR}}e^{i\phi_{\text{NR}}} + \sum_r a_r e^{i\phi_r} A_r(s_+, s_-)]/N_f$, where the first term represents a nonresonant contribution, the sum is over all intermediate two-body resonances *r*, and N_f is such that $\int ds_+ ds_- |f(s_+, s_-)|^2 = 1$. The amplitude for the decay chain $D^0 \rightarrow rC$, $r \rightarrow AB$ is $A_r(s_+, s_-) = F_r F_s [m_r^2 - M_{AB}^2 - im_r \Gamma_r(M_{AB})]^{-1}$, where m_r is the peak

mass of the resonance [11], M_{AB}^2 is the squared invariant mass of the AB pair, F_r is a spin-dependent form factor [12], and $\Gamma_r(M_{AB})$ is the mass-dependent width for the resonance r [12]. The spin factors F_s are $F_0 = m_D^2$, $F_1 = M_{BC}^2 - M_{AC}^2 + (m_D^2 - m_C^2)(m_A^2 - m_B^2)M_{AB}^{-2}$, and $F_2 = (F_1^2 - \frac{1}{3}\mu_{CD}^2\mu_{AB}^2)m_D^{-2}$, where $\mu_{jk}^2 \equiv M_{AB}^2 - 2m_j^2 - 2m_k^2 + (m_j^2 - m_k^2)^2M_{jk}^{-2}$, and m_i is the mass of particle i [11].

In step 1, we determine the parameters a_{NR} , a_r , ϕ_{NR} , and ϕ_r by fitting a large sample of D^0 and \bar{D}^0 mesons, flavor tagged through their production in the decay $D^{*+} \rightarrow D^0\pi^+$ [13]. To select this sample, we require the c.m. momentum of the D^* candidate to be greater than 2770 MeV/ c , and $|M_{D^*} - M_D - 145.4 \text{ MeV}/c^2| < 0.6 \text{ MeV}/c^2$, where M_{D^*} is the invariant mass of the D^* candidate. The signal and background yields are obtained from a fit to the M_D distribution, modeling the signal as a Gaussian and the background as an exponential. The signal Gaussian peaks at $1863.7 \pm 0.4 \text{ MeV}/c^2$ and has a width of $17.4 \pm 0.8 \text{ MeV}/c^2$.

Of the D^0 candidates in the signal region $1848 < M_D < 1880 \text{ MeV}/c^2$, we obtain from the fit $N_S = 44780 \pm 250$ signal and $N_B = 830 \pm 70$ background events. To obtain the parameters of $f(s_+, s_-)$, we fit these candidates with the probability distribution function (PDF) $N_S|f(s_+, s_-)|^2\epsilon(s_+, s_-) + N_B|f_B(s_+, s_-)|^2$, where the background PDF $f_B(s_+, s_-)$ is a binned distribution obtained from events in the sideband $1930 < M_D < 1990 \text{ MeV}/c^2$, and $\epsilon(s_+, s_-)$ is an efficiency function, parametrized as a two-dimensional third-order polynomial determined from MC. To within the MC-signal statistical

uncertainty, $\epsilon(s_+, s_-) = \epsilon(s_-, s_+)$. The region $M_D < 1848 \text{ MeV}/c^2$, which contains $D^0 \rightarrow K^-\pi^+\pi^0$ events that are absent from the signal region, is not used.

Table I summarizes the results of this fit, with systematic errors obtained by varying the masses and widths of the $\rho(1700)$ and σ resonances, setting $F_r = 1$, and varying $\epsilon(s_+, s_-)$ to account for uncertainties in reconstruction and particle identification. The Dalitz plot distribution of the data is shown in Fig. 1(a). The distribution is marked by three destructively interfering $\rho\pi$ amplitudes, suggesting an $I = 0$ -dominated final state [14].

The fit for step $i \in \{2, 3\}$ uses the PDF

$$\mathcal{P}_i^C = \sum_t \frac{N_t}{2\eta} (1 - CA_t) \mathcal{P}_{i,t}^{(C)}(\xi_i) / \int \mathcal{P}_{i,t}^{(C)}(\xi_i) d^{n_i} \xi_i, \quad (1)$$

where ξ_i is the set of n_i event variables $\xi_2 = \{\Delta E, q', d'\}$, $\xi_3 = \{\Delta E, q', s_-, s_+\}$, t corresponds to one of the ten event types listed above, $N_t = N_t^+ + N_t^-$ is the number of events of type t , $A_t = (N_t^- - N_t^+)/N_t$ is their charge asymmetry, $C = \pm 1$ is the electric charge of the B candidate, and $\eta \equiv \sum_t N_t$. Using MC, we verify that the variables in each set ξ_i are uncorrelated for each event type. Therefore, the PDFs $\mathcal{P}_{i,t}^{(C)}$ are the products

$$\mathcal{P}_{2,t}(\Delta E, q', d') = \mathcal{E}_t(\Delta E) \mathcal{Q}_t(q') \mathcal{C}_t(d'), \quad (2)$$

$$\mathcal{P}_{3,t}^C(\Delta E, q', s_+, s_-) = \mathcal{E}_t(\Delta E) \mathcal{Q}_t(q') \mathcal{D}'_t^C(s_+, s_-).$$

The parameters of the Dalitz plot PDF $\mathcal{D}'_{DK_{\text{sig}}}^C(s_+, s_-)$ are obtained from the data as described below. Those of all other functions in Eq. (2) are obtained from the MC samples. The functions $\mathcal{E}_t(\Delta E)$ are parametrized as the

TABLE I. Result of the fit to the $D^{*+} \rightarrow D^0\pi^+$ sample, showing the amplitudes ratios $R_r \equiv a_r/a_{\rho^+(770)}$, phase differences $\Delta\phi_r \equiv \phi_r - \phi_{\rho^+(770)}$, and fit fractions $f_r \equiv \int |a_r A_r(s_+, s_-)|^2 ds_- ds_+$. The first (second) errors are statistical (systematic). We take the mass (width) of the σ meson to be 400(600) MeV/ c^2 .

State	R_r (%)	$\Delta\phi_r$ ($^\circ$)	f_r (%)
$\rho^+(770)$	100	0	$67.8 \pm 0.0 \pm 0.6$
$\rho^0(770)$	$58.8 \pm 0.6 \pm 0.2$	$16.2 \pm 0.6 \pm 0.4$	$26.2 \pm 0.5 \pm 1.1$
$\rho^-(770)$	$71.4 \pm 0.8 \pm 0.3$	$-2.0 \pm 0.6 \pm 0.6$	$34.6 \pm 0.8 \pm 0.3$
$\rho^+(1450)$	$21 \pm 6 \pm 13$	$-146 \pm 18 \pm 24$	$0.11 \pm 0.07 \pm 0.12$
$\rho^0(1450)$	$33 \pm 6 \pm 4$	$10 \pm 8 \pm 13$	$0.30 \pm 0.11 \pm 0.07$
$\rho^-(1450)$	$82 \pm 5 \pm 4$	$16 \pm 3 \pm 3$	$1.79 \pm 0.22 \pm 0.12$
$\rho^+(1700)$	$225 \pm 18 \pm 14$	$-17 \pm 2 \pm 3$	$4.1 \pm 0.7 \pm 0.7$
$\rho^0(1700)$	$251 \pm 15 \pm 13$	$-17 \pm 2 \pm 2$	$5.0 \pm 0.6 \pm 1.0$
$\rho^-(1700)$	$200 \pm 11 \pm 7$	$-50 \pm 3 \pm 3$	$3.2 \pm 0.4 \pm 0.6$
$f_0(980)$	$1.50 \pm 0.12 \pm 0.17$	$-59 \pm 5 \pm 4$	$0.25 \pm 0.04 \pm 0.04$
$f_0(1370)$	$6.3 \pm 0.9 \pm 0.9$	$156 \pm 9 \pm 6$	$0.37 \pm 0.11 \pm 0.09$
$f_0(1500)$	$5.8 \pm 0.6 \pm 0.6$	$12 \pm 9 \pm 4$	$0.39 \pm 0.08 \pm 0.07$
$f_0(1710)$	$11.2 \pm 1.4 \pm 1.7$	$51 \pm 8 \pm 7$	$0.31 \pm 0.07 \pm 0.08$
$f_2(1270)$	$104 \pm 3 \pm 21$	$-171 \pm 3 \pm 4$	$1.32 \pm 0.08 \pm 0.10$
$\sigma(400)$	$6.9 \pm 0.6 \pm 1.2$	$8 \pm 4 \pm 8$	$0.82 \pm 0.10 \pm 0.10$
Nonresonant	$57 \pm 7 \pm 8$	$-11 \pm 4 \pm 2$	$0.84 \pm 0.21 \pm 0.12$

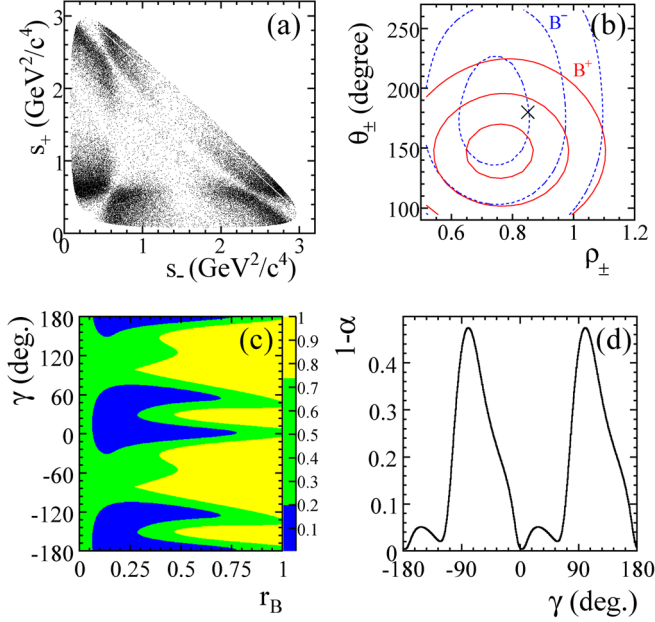


FIG. 1 (color online). (a) The two-dimensional (s_+ , s_-) distribution of the $D^{*+} \rightarrow D^0 \pi^+$ data. Charge conjugation is implied. (b) One-, two-, and three-standard-deviation contours of \mathcal{L} as functions of θ_{\pm} vs ρ_{\pm} . The solid (dashed) curves correspond to B^+ (B^-) results. The no-interference point ($\rho_{\pm} = x_0$, $\theta_{\pm} = 180^\circ$) is marked with an \times . (c) Projection of the three-dimensional confidence level $1 - \alpha$ onto r_B and γ . (d) $1 - \alpha$ vs γ .

sum of a Gaussian and a second-order polynomial. The PDFs $\mathcal{Q}_i(q')$ and $\mathcal{C}_i(d')$ are the sum of a Gaussian and an asymmetric Gaussian. The PDF parameters are different for each event type. Assuming no CP violation in the background, we take $\mathcal{D}'_i^+(s_+, s_-) = \mathcal{D}'_i^-(s_-, s_+)$ and $A_i = 0$ for $t \neq DK_{\text{sig}}$. The functions $\mathcal{D}'_{D\pi X}^C(s_+, s_-)$ and $\mathcal{D}'_{DK_{\text{bgd}}}^C(s_+, s_-)$ are binned histograms obtained from the MC. For other event types, $\mathcal{D}'_i^C(s_+, s_-) = \epsilon(s_+, s_-)\mathcal{D}'_i^C(s_+, s_-)$, where the efficiency function $\epsilon(s_+, s_-)$ has different parameters for well-reconstructed and misreconstructed D candidates.

We define $z_{\pm} \equiv r_B e^{i(\delta \pm \gamma)}$, where δ is a CP -even phase and r_B is the ratio of the magnitudes of the $b \rightarrow u\bar{c}s$ and $b \rightarrow c\bar{u}s$ amplitudes. Ignoring negligible D^0 - \bar{D}^0 mixing effects [15], the signal Dalitz PDF is

$$\mathcal{D}_{DK_{\text{sig}}}^{\pm}(s_+, s_-) = |f(s_{\mp}, s_{\pm}) + z_{\pm} f(s_{\pm}, s_{\mp})|^2. \quad (3)$$

In the step-2 fit, we extract the $B^{\pm} \rightarrow D_{\pi^+ \pi^- \pi^0} K^{\pm}$ signal yield and asymmetry, as well as some background yields, as described in Ref. [10]. From this fit we find $N_{DK_{\text{sig}}} = 170 \pm 29$ signal events, corresponding to the branching fraction $\mathcal{B}(B^{\pm} \rightarrow D_{\pi^+ \pi^- \pi^0} K^{\pm}) = (4.6 \pm 0.8 \pm 0.4) \times 10^{-6}$, and the decay rate asymmetry $A_{DK_{\text{sig}}} = -0.02 \pm 0.15 \pm 0.03$. The first errors are statistical and the second are systematic, due to sources described below.

Only the complex parameters z_{\pm} are free in the step-3 fit. This fit minimizes the function

$$\mathcal{L} = - \sum_{e=1}^{N_{\text{ev}}} \log \mathcal{P}_3^{C_e}(\xi_3^e) + \frac{1}{2} \chi^2, \quad (4)$$

where N_{ev} is the number of events in the data sample. The term $\chi^2 = \sum_{u,v=1}^2 X_u V_{uv}^{-1} X_v$ increases the sensitivity of the fit by using the results of the step-2 fit via $X_1 = N_{DK_{\text{sig}}} - (n_- + n_+)$ and $X_2 = A_{DK_{\text{sig}}} - (n_- - n_+) / (n_- + n_+)$, where

$$n_{\pm} = N^0 \frac{\int \mathcal{D}_{DK_{\text{sig}}}^{\pm}(s_+, s_-) ds_+ ds_-}{\int |f(s_{\mp}, s_{\pm})|^2 \epsilon(s_+, s_-) ds_+ ds_-} \quad (5)$$

are the expected numbers of B^{\pm} signal events. In Eq. (5), N^0 is the product of the number $N_{B^+ B^-}$ of charged $B^+ B^-$ pairs in the data set, the branching fractions $\mathcal{B}(B^- \rightarrow D^0 K^-)$ [11] and $\mathcal{B}(D^0 \rightarrow \pi^+ \pi^- \pi^0)$ [13], and the reconstruction efficiency ϵ . The error matrix V_{uv} is the sum of two components: the step-2 fit error matrix V_{uv}^{stat} , which is almost diagonal (the correlation coefficient is -2.8%), and the N^0 systematic error matrix V_{uv}^{sys} . Here $V_{12}^{\text{sys}} = V_{22}^{\text{sys}} = 0$, and $V_{11}^{\text{sys}} = \sum_{c=1}^4 (N^0 \sigma_c^{\text{rel}})^2$, where σ_c^{rel} are the relative errors on the four components $N_{B^+ B^-}$ (1.1%), ϵ (3.3%), $\mathcal{B}(D \rightarrow \pi^+ \pi^- \pi^0)$ (3.8%) [13], and $\mathcal{B}(B^- \rightarrow D^0 K^-)$ (5.9%) [11].

We parametrize z_{\pm} with the polar coordinates

$$\rho_{\pm} \equiv |z_{\pm} - x_0|, \quad \theta_{\pm} \equiv \tan^{-1} \left(\frac{\text{Im}[z_{\pm}]}{\text{Re}[z_{\pm}] - x_0} \right), \quad (6)$$

where the parameter $x_0 = 0.85$ is obtained from

$$x_0 \equiv - \int \text{Re}[f(s_+, s_-) f^*(s_-, s_+)] \epsilon(s_+, s_-) ds_+ ds_-. \quad (7)$$

This parametrization is optimal due to the polar symmetry of $n_{\pm} = N^0(1 + \rho_{\pm}^2 - x_0^2)$, and avoids nonlinear correlations and biases that occur with the parametrizations (r_B , γ , δ) or ($\text{Re}[z_{\pm}]$, $\text{Im}[z_{\pm}]$). The step-3 fit yields

$$\begin{aligned} \rho_- &= 0.72 \pm 0.11 \pm 0.04 \pm 0.05, \\ \theta_- &= (173 \pm 42 \pm 2 \pm 19)^\circ, \\ \rho_+ &= 0.75 \pm 0.11 \pm 0.04 \pm 0.05, \\ \theta_+ &= (147 \pm 23 \pm 1 \pm 13)^\circ, \end{aligned} \quad (8)$$

where the first errors are statistical, the second are due to V_{11}^{sys} , and the third are due to additional systematic errors, described below. The largest correlation coefficient is $c_{\rho-\rho_+} = 14\%$, originating from V_{11}^{sys} . All others are 1% or less. Contours of constant \mathcal{L} values are shown in Fig. 1(b).

The third errors in Eq. (8) and the systematic errors on $\mathcal{B}(B^\pm \rightarrow D_{\pi^+\pi^-\pi^0} K^\pm)$ and $A_{DK_{\text{sig}}}$ are obtained as follows. The uncertainty in the model used for $f(s_+, s_-)$ is the largest source of error on the CP parameters: $\sigma_{\rho_\pm}^{\text{model}} = 0.03$, $\sigma_{\theta_-}^{\text{model}} = 14^\circ$, $\sigma_{\theta_+}^{\text{model}} = 11^\circ$. This error is evaluated by removing all but the $\rho(770)$, $\rho(1450)$, $f_0(980)$, and nonresonant terms in $f(s_+, s_-)$, adding an $f_2'(1525)$, an ω , and a nonresonant P -wave contribution, varying the meson “radius” parameter in F_r [12], and propagating the errors from Table I. Uncertainties due to the masses and widths of the $\rho(1700)$ and σ resonances are small by comparison. Other errors are due to uncertainties on background yields that are fixed in the fits [10], the finite MC sample size, a possible reconstruction efficiency charge asymmetry, and uncertainties in the background PDF shapes, evaluated by comparing MC and data in signal-free sidebands of the variables M_D , ΔE , and m_{ES} . We also evaluate errors due to possible charge asymmetries in DKX and DK_{bgd} events, uncertainties in particle identification and the efficiency functions, the finite s_\pm measurement resolution, the background PDF f_B in the D^* sample, D -flavor mistagging in the D^* sample, and correlations between the D flavor and the kaon charge in qq_D events.

The analysis procedure is validated in several ways. Conducting the analysis on the MC sample yields results consistent with the generated values. We carry out the step-3 fit on a sample of $1800 \pm 70 B^- \rightarrow D_{\pi^+\pi^-\pi^0}^- \pi^-$ events, obtaining the background Dalitz plot distribution from the ΔE sideband. The fit yields $\rho_- = 0.815 \pm 0.034$, $\theta_- = (186 \pm 7)^\circ$, $\rho_+ = 0.854 \pm 0.035$, $\theta_+ = (192 \pm 7)^\circ$, consistent with $\rho_\pm = x_0$, $\theta_\pm = 180^\circ$, which corresponds to $z_\pm = 0$. We verify the signal efficiency by measuring the branching fraction $\mathcal{B}(B^- \rightarrow D^0 \pi^-)$ with $D^0 \rightarrow K^- \pi^+ \pi^0$ and $D^0 \rightarrow \pi^+ \pi^- \pi^0$. We compare the fit variable distributions of data and MC events in signal-free sidebands. Good agreement is found in all cases.

We use the frequentist approach outlined in Ref. [6] to extract confidence regions of $\mathbf{p} = (r_B, \gamma, \delta)$, accounting for the dependence of the experimental errors on the values of z_\pm and for small non-Gaussian effects in the likelihood function. Two-dimensional projections onto r_B and γ of regions of one, two, and three standard deviations (σ) are shown in Fig. 1(c). These regions are defined as containing the \mathbf{p} values with three-dimensional significance α smaller than 19.9%, 73.9%, and 97.1%, respectively. Figure 1(d) shows the projected γ dependence of the confidence level $1 - \alpha$. We find the one- σ regions

$$\begin{aligned} 0.06 < r_B < 0.78, \quad -30^\circ < \gamma < 76^\circ, \\ -27^\circ < \delta < 78^\circ, \end{aligned} \quad (9)$$

including both statistical and systematic errors. Sensitivity

to r_B , γ , and δ arises from both the Dalitz plot distribution and the signal branching fraction and asymmetry.

We are grateful for the excellent luminosity and machine conditions provided by our PEP-II colleagues, and for the substantial dedicated effort from the computing organizations that support *BABAR*. The collaborating institutions wish to thank SLAC for its support and kind hospitality. This work is supported by DOE and NSF (USA), NSERC (Canada), IHEP (China), CEA and CNRS-IN2P3 (France), BMBF and DFG (Germany), INFN (Italy), FOM (The Netherlands), NFR (Norway), MIST (Russia), MEC (Spain), and PPARC (United Kingdom). Individuals have received support from the Marie Curie EIF (European Union) and the A. P. Sloan Foundation.

*Deceased.

†Now at Tel Aviv University, Tel Aviv, 69978, Israel.

‡Also with Dipartimento di Fisica, Università di Perugia, Perugia, Italy.

§Also with Università della Basilicata, Potenza, Italy.

||Also with IPPP, Physics Department, Durham University, Durham DH1 3LE, United Kingdom.

- [1] N. Cabibbo, Phys. Rev. Lett. **10**, 531 (1963); M. Kobayashi and T. Maskawa, Prog. Theor. Phys. **49**, 652 (1973).
- [2] M. Gronau and D. Wyler, Phys. Lett. B **265**, 172 (1991).
- [3] A. Giri, Y. Grossman, A. Soffer, and J. Zupan, Phys. Rev. D **68**, 054018 (2003); A. Bondar, “Proceedings of BINP Special Analysis Meeting on Dalitz Analysis” (unpublished).
- [4] We use the symbol D to indicate any linear combination of a D^0 and a \bar{D}^0 meson state.
- [5] A. Poluektov *et al.* (Belle Collaboration), Phys. Rev. D **73**, 112009 (2006).
- [6] B. Aubert *et al.* (*BABAR* Collaboration), Phys. Rev. Lett. **95**, 121802 (2005).
- [7] Y. Grossman, Z. Ligeti, and A. Soffer, Phys. Rev. D **67**, 071301(R) (2003).
- [8] See “Fit A” in D. Cronin-Hennessy *et al.* (CLEO Collaboration), Phys. Rev. D **72**, 031102 (2005).
- [9] B. Aubert *et al.* (*BABAR* Collaboration), Nucl. Instrum. Methods Phys. Res., Sect. A **479**, 1 (2002).
- [10] B. Aubert *et al.* (*BABAR* Collaboration), Phys. Rev. D **72**, 071102 (2005).
- [11] Y.-M. Yao *et al.* (Particle Data Group), J. Phys. G **33**, 1 (2006).
- [12] See Eq. (5) and Table 1 in S. Kopp *et al.* (CLEO Collaboration), Phys. Rev. D **63**, 092001 (2001).
- [13] B. Aubert *et al.* (*BABAR* Collaboration), Phys. Rev. D **74**, 091102 (2006).
- [14] C. Zemach, Phys. Rev. **133**, B1201 (1964).
- [15] Y. Grossman, A. Soffer, and J. Zupan, Phys. Rev. D **72**, 031501(R) (2005).